Tracing the location of the reconnection site from the northern and southern cusps

K. J. Trattner,[1] S. M. Petrinec,[1] W. K. Peterson,[2] S. A. Fuselier,[1] and H. Reme[3]

Received 15 February 2006; revised 15 August 2006; accepted 21 August 2006; published 9 November 2006.

[1] Three-dimensional plasma observations in the cusp have been successfully used to investigate the location of the reconnection site at the magnetopause. This technique uses low-velocity cutoffs in the precipitating and mirrored magnetosheath population traveling along open cusp field lines, which are then used to estimate the distance to the reconnection line. This distance is subsequently traced back along model magnetic field lines to the magnetopause to identify the location of the reconnection site. In this paper we use data obtained from two widely spaced spacecraft to assess the robustness and consistency in identifying the reconnection site using this technique. Two cusp crossings on 3 March 2003, observed by the Cluster satellites in the Northern Hemisphere and the Polar spacecraft in the Southern Hemisphere during similar solar wind plasma and IMF conditions, are used to trace the location of the reconnection site from two directions. Both estimates point to a reconnection site in the Southern Hemisphere close to the antiparallel reconnection site. The distributions of the trace locations at the magnetopause suggest the existence of a tilted X-line which crosses that region for these solar wind plasma and interplanetary magnetic field conditions, but the distinction between the antiparallel and the component reconnection scenario could not be conclusively made.

Citation: Trattner, K. J., S. M. Petrinec, W. K. Peterson, S. A. Fuselier, and H. Reme (2006), Tracing the location of the reconnection site from the northern and southern cusps, *J. Geophys. Res.*, *111*, A11211, doi:10.1029/2006JA011673.

1. Introduction

[2] The concept of magnetic reconnection of the interplanetary magnetic field (IMF) with the geomagnetic field was originally postulated by *Dungey* [1961] to explain the inferred circulation of magnetic flux and plasma in the outer magnetosphere and high-latitude ionosphere. Reconnection was assumed to occur between magnetic field lines of exactly opposite polarity and is referred to as antiparallel reconnection [e.g., *Gosling et al.*, 1991]. Recent results have shown that reconnection can also occur for nonantiparallel magnetic field orientations. Currently, one of the major outstanding questions about magnetic reconnection at the magnetopause is where reconnection will occur as a function of the orientation of the IMF.

[3] For purely southward IMF, antiparallel reconnection between the IMF and magnetospheric field lines should occur near the subsolar magnetopause [e.g., *Aubry et al.*, 1970; *Fairfield*, 1971; *Fuselier et al.*, 1991; *Petrinec and Fuselier*, 2003; *Phan et al.*, 1996]. If the IMF is southward and a B_Y component is present, the antiparallel region bifurcates at the noon-midnight meridian and is located at midlatitudes [*Crooker*, 1979; *Luhmann et al.*, 1984]. Antiparallel reconnection for magnetospheric field lines, for times when the IMF is northward, should occur at the high-latitude magnetopause in the lobes, poleward of the cusps, with IMF field lines draped around the magnetopause [*Dungey*, 1963; *Fuselier et al.*, 2000].

[4] Reconnection has also been inferred in regions where the magnetic fields are not antiparallel. In general, magnetic reconnection in regions where the field lines are not antiparallel is labeled as component reconnection, and magnetic shear angles as low as 50° have been reported [e.g., *Gosling et al.*, 1990]. During southward IMF conditions, component reconnection is thought to occur along a tilted neutral line which passes through the subsolar magnetopause [e.g., *Sonnerup*, 1974; *Cowley*, 1976; *Sonnerup et al.*, 1981; *Cowley and Owen*, 1989; *Fuselier et al.*, 2002]. Antiparallel and component reconnection scenarios lead to significantly different reconnection sites and plasma transfer rates.

[5] A statistical study by *Trattner et al.* [2004] on the location of the reconnection line for 52 Polar cusp crossings during northward IMF conditions revealed an approximately equal probability for antiparallel and component reconnection between the IMF and the magnetospheric field. Of special interest in this study were events during the same IMF conditions for which precipitating ion signatures typical of magnetic reconnection could be observed in the dawn and dusk sectors. These events revealed that the observed reconnection scenario, antiparallel or component, depends only on the location of the satellite, either in a region mapping to the antiparallel reconnection site or to the

[1]Lockheed Martin Advanced Technology Center, Palo Alto, California, USA.
[2]Laboratory for Atmospheric and Space Physics, University of Colorado, Boulder, Colorado, USA.
[3]Centre d'Etude Spatiale des Rayonnements, Toulouse, France.

0148-0227/06/2006JA011673

component reconnection site. It was concluded that the reconnection line during northward IMF conditions extends from a rather small antiparallel reconnection site into regions where the magnetic fields are no longer strictly antiparallel. The antiparallel and component reconnection scenarios occur simultaneously along the same reconnection line.

[6] Consistent with this study, *Onsager et al.* [2001] reported the existence of a very long reconnection line for an event observed during high solar wind dynamic pressure conditions. For this event, open magnetic field lines within the high-latitude magnetosphere were observed, while the IMF remained relatively constant and the satellite position changed location from 1000 to 1630 MLT. Since the extent of the antiparallel reconnection site at the high-latitude magnetopause during northward IMF conditions is relatively small, the large local time coverage indicates that antiparallel and component reconnection would be most probably occurring simultaneously.

[7] Ionosphere observations by the FUV instrument on board the Imager for Magnetopause to Aurora Global Exploration (IMAGE) spacecraft can be used directly to distinguish between the antiparallel or component reconnection sites. The emissions observed by IMAGE/FUV are caused by precipitating ions with high number flux and energies above about 2 keV. Several examples for southward IMF conditions with a significant B_y component show that IMAGE/FUV emissions from a component reconnection site (tilted X-line) will form a continuous band along the auroral oval over a wide local time range [*Fuselier et al.*, 2002]. On the other hand, emissions from the antiparallel reconnection sites create dayside auroral emissions with a gap close to one or the other side of local noon [e.g., *Petrinec and Fuselier*, 2003].

[8] *Trattner et al.* [2005] used a double-cusp event observed by the Cluster satellites to determine the location of the reconnection sites for the two ion-energy dispersions. The two-cusp structures have been identified previously as spatial cusp structures associated with the dawn and dusk convection cells. The low-velocity cutoff technique was used to calculate the distance between the satellites and the reconnection lines. Analysis showed that the two cusp structures map to two reconnection lines in different hemispheres consistent with the antiparallel reconnection model.

[9] It is the purpose of this study to demonstrate the accuracy of the low-velocity cutoff technique by estimating the location of the reconnection site from satellites located in different hemispheres. Two cusp crossings in the Southern and Northern Hemispheres by the Polar and Cluster SC1 spacecraft, respectively, have been selected. Both crossings occurred on 3 March 2003, during similar IMF conditions, about 8 hours apart in universal time. Three-dimensional ion measurements from the Toroidal Imaging Mass-Angle Spectrograph (TIMAS) on Polar and the Cluster Ion Spectrometers (CIS) on Cluster are used to estimate the distance to the reconnection site and subsequently trace this distance back to the magnetopause along geomagnetic field lines. The Cluster trace from the Northern Hemisphere and the Polar trace from the Southern Hemisphere point to the same region in the dusk sector of the Southern Hemisphere, close to the antiparallel reconnection region, demonstrating the robustness of the low-velocity cutoff technique. Despite being close to the antiparallel reconnection site, the distribution of the reconnection traces on the magnetopause lead to the conclusion that these cases are consistent with a tilted X-line across the subsolar point.

2. Instrumentation and Methodology

[10] In this paper we present proton observations from a Southern Hemisphere cusp using the TIMAS instrument [*Shelley et al.*, 1995] on board the Polar spacecraft. Polar/TIMAS proton measurements cover the energy range from 15 eV/e to 33 keV/e and provide 98% coverage of the unit sphere during a 6-s spin period. The Polar spacecraft was launched on 24 February 1996, into a nearly 90° inclination orbit with a perigee of about 2 R_E and an apogee of about 9 R_E. While the initial Polar orbit had an apogee over the northern polar region, it has precessed in latitude such that apogee in 2003 is over the southern polar region, providing a unique opportunity for conjugate cusp studies together with the Cluster mission. Polar crosses the cusp during two periods each year, with each period lasting for several months. The cusp ion distributions are observed at altitudes between 3.5 and 9 R_E in the cusp and up to 90° invariant latitude (ILAT).

[11] Four identical Cluster satellites were launched in pairs on 15 July and 9 August 2000, into orbits with a perigee of $\sim$4 R_E, an apogee of $\sim$19.7 R_E and an inclination of 90°. The Cluster satellites carry the Cluster Ion Spectrometers (CIS) [*Reme et al.*, 2001] that provide high-precision three-dimensional (3-D) distributions for the major ion species at energies from about 20 eV to about 40 keV/e every 4 s (1 spin period) in the high time resolution mode. The CIS instruments consist of two different analyzers, the Hot Ion Analyzer (HIA) and the time-of-flight Composition and Distribution Function Analyzer (CODIF). This study will focus on proton observations by the CODIF instrument on board SC1. Data from the CODIF instrument on SC3 recorded only partial three-dimensional distributions while the SC4 satellite did not encounter clearly defined cusp ion energy structures, which are necessary to provide valid, widely separated low-velocity cutoffs needed for the technique. The observations from SC3 and SC4 are therefore omitted from this study.

[12] Ion observations in the cusp exhibit a so-called time-of-flight effect. For a southward IMF, newly opened field lines convect poleward under the joint action of magnetic tension and shocked solar wind flow, causing a time dispersion whereby particles of decreasing energy arrive at successively higher latitudes [e.g., *Rosenbauer et al.*, 1975; *Shelley et al.*, 1976]. This kinematic effect gives rise to distinctive ion energy-latitude dispersions [e.g., *Reiff et al.*, 1977; *Smith and Lockwood*, 1996]. By using the time-of-flight effect and the three-dimensional capability of the ion detectors, it is possible to estimate the distance from the observing satellite to the reconnection line X_r defined by:

$$X_r/X_m = 2\,V_e/(V_m - V_e) \quad (1)$$

where X_m is the distance to the ionospheric mirror point, V_e is the cutoff velocity of the precipitating (earthward propagating) ions, and V_m is the cutoff velocity of the mirrored distribution [e.g., *Onsager et al.*, 1990; *Fuselier et*

al., 2000]. X_m is determined by using the position of the Polar or Cluster SC1 spacecraft in the cusp and tracing the geomagnetic field line at this position down to the ionosphere by using the Tsyganenko 1996 (T96) model [*Tsyganenko*, 1995]. The low-velocity cutoff velocities V_e and V_m are determined from the three-dimensional proton distribution observed in the cusp.

[13] We note that the distance to the reconnection line outlined in equation (1) could be affected by time varying electric fields directed along the reconnected magnetic field line. The influence of such electric fields and their effects depend upon the exact time-dependent formulation of the electric and magnetic fields which is beyond the scope of this paper. This study assumes that no electric fields directed along the reconnected field lines are present. However, in a static situation, since the electric field is conservative, any positive acceleration of plasma in the earthward direction due to a parallel electric field is countered by a negative acceleration of plasma in the upward direction. The time-of-flight equation for estimating the location of reconnection would be unaffected.

[14] In addition to Polar and Cluster data, IMF and the solar wind conditions were observed by the ACE Magnetic Field Instrument (MFI) [*Smith et al.*, 1998] and the ACE Solar Wind Experiment (SWE) [*McComas et al.*, 1998], respectively. The IMF and solar wind data are provided by the ISTP key parameter Web page.

3. Observations

[15] The location of the reconnection line at the magnetopause would be ideally determined by crossing the reconnection region with a satellite. This scenario is not easy to achieve since, depending on the solar wind conditions, the reconnection site will move to different locations. In addition, most spacecraft cross the magnetopause only at a single point, which severely limits the chance to encounter the actual reconnection site. This limitation in covering larger areas of the magnetopause surface will be addressed with the currently planned Magnetospheric Multiscale (MMS) mission; the orbit is configured to skim along the nominal dayside magnetopause.

[16] Simultaneous multipoint measurements at the magnetopause are able to address some of the shortcomings. For more than 1 hour on 11 February 1998, the trajectories of both Equator-S and Geotail skimmed the dawn flank magnetopause at low latitudes and observed bidirectional ion jets. *Phan et al.* [2000] interpreted the existence of these bidirectional ion jets as evidence of substantial entry of the solar wind into the magnetosphere at a stable and extended reconnection line located between the satellites.

[17] A further method of locating the reconnection line was introduced by *Fuselier et al.* [2005]. Using 3-D plasma observations of two Cluster spacecraft, the technique provides under some restrictive assumptions and conditions a snapshot of the reconnection inflow velocity into the magnetosphere and an estimate of the distance from the spacecraft to the reconnection site.

[18] In this study we demonstrate the accuracy of the low-velocity cutoff method applied to 3-D plasma observations in the cusp. Cusp crossings by the Polar satellite in the Southern Hemisphere and the Cluster satellites in the Northern Hemisphere have been selected to trace the distance to the reconnection line from opposite locations. These separate events have been selected because of their proximity in time and especially their similar solar wind and IMF conditions. While cusp crossings in different hemispheres at the same time would be the ideal scenario, similar solar wind and IMF conditions are known to cause the magnetosphere to respond in a similar way. In a multispacecraft study to investigate the temporal or spatial nature of cusp structures, *Trattner et al.* [2002b] demonstrated that unrelated cusp crossings observed during similar and stable solar wind and IMF conditions exhibit spatial cusp features with similar profiles. These observations showed that magnetospheric reconnection at the magnetopause responds in a directly comparable and predictable way to similar outside conditions, and in general the shear angles across the magnetopause should also be similar. If the particle tracing method is robust, reconnection regions at the magnetopause should be identified at similar locations even if traced from widely separated satellites. This allows for a direct comparison of the location of the reconnection line for these two cusp crossings.

[19] The Polar cusp crossing on 3 March 2003 occurred from 0110 UT to 0130 UT. The orbit locations of the Polar and Cluster satellites for this time period together with the T96 magnetosphere for the observed solar wind conditions are shown in Figure 1 (left). While the Polar satellite (blue) crossed the southern cusp the Cluster satellites (black (SC1), red (SC2), green (SC3), and magenta (SC4)) are located in the southern magnetospheric tail. During the Polar cusp crossing, the solar wind density was about 10 cm^{-3} and the solar wind velocity was 380 km/s. The IMF components were stable with only minor fluctuations. Their average conditions are (4.9, −3.6, −1.2) nT in GSM coordinates, which results in an IMF clock angle of 252°.

[20] The Cluster cusp crossing on 3 March 2003 occurred from 0900 UT to 1100 UT. The orbit locations for this time interval are shown in Figure 1 (right) with the Cluster satellites in the northern cusp and the Polar satellite in the dayside equatorial region. During the Cluster cusp crossing the solar wind density was about 12 cm^{-3} and the solar wind velocity was 380 km/s. Similar to the Polar cusp crossing, the IMF conditions were stable with minor fluctuations. Their average conditions during the time of interest (see Figure 2) were (5.2, −5.8, −1) nT in GSM coordinates, which results in an clock angle of about 260°.

[21] The difference in clock angle between the two cusp crossings is just 8° with about the same dynamic pressure. For both cusp crossings the solar wind and IMF conditions were observed by the ACE spacecraft and have been propagated by 1 hour and 4 min to account for the travel time to the magnetopause.

[22] Figure 2 shows H^+ omnidirectional flux measurements (1/(cm^2 s sr keV/e), observed by the CIS instrument on board Cluster SC1 during the 3 March 2003 northern cusp crossing. Cluster was located at about 77° ILAT, 7.9 R_E geocentric altitude and in the afternoon sector at 1310 magnetic local time (MLT). The satellite was moving from the polar region towards the magnetopause, and to higher altitudes as it crossed into the magnetosheath at about 1007 UT (marked by a vertical white line) without encountering the equatorward located ion open-closed field line

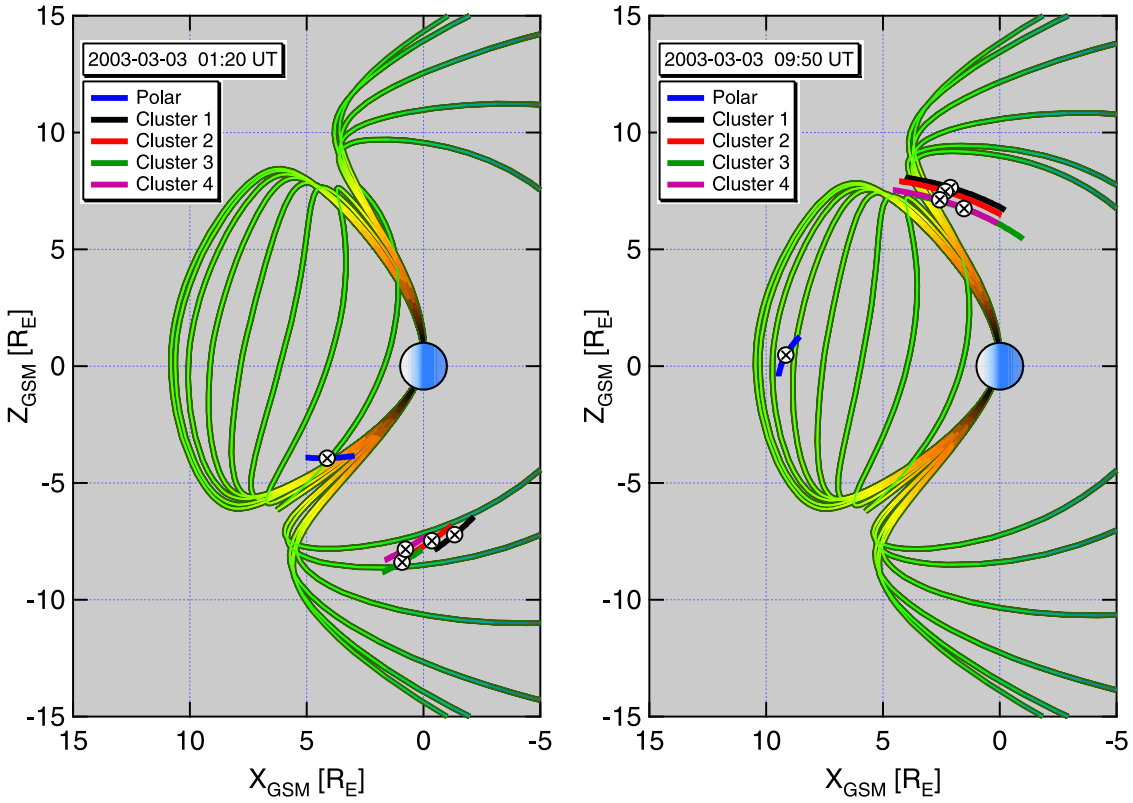

Figure 1. Orbit locations of the Polar and Cluster satellites during the two cusp events on 3 March 2003. The Polar satellite (blue) crossed the southern cusp (left) from 0110 to 0128 UT while the Cluster satellite SC1 (black) crossed the northern cusp from 0900 to 1005 UT. Similar interplanetary magnetic field (IMF) conditions have been reported by the ACE spacecraft for both cusp crossings, which allows for a direct comparison of the location of the reconnection sites.

boundary. During the cusp crossing, Cluster encountered a typical ion energy dispersion for southward IMF, with the precipitating ion energy increasing with decreasing invariant latitude. This dispersion is the direct result of the time-of-flight or velocity filter effect produced by the merging and subsequent sunward convection of the reconnected magnetic field lines [e.g., *Rosenbauer et al.*, 1975; *Onsager et al.*, 1993]. The cusp crossing also shows several sudden

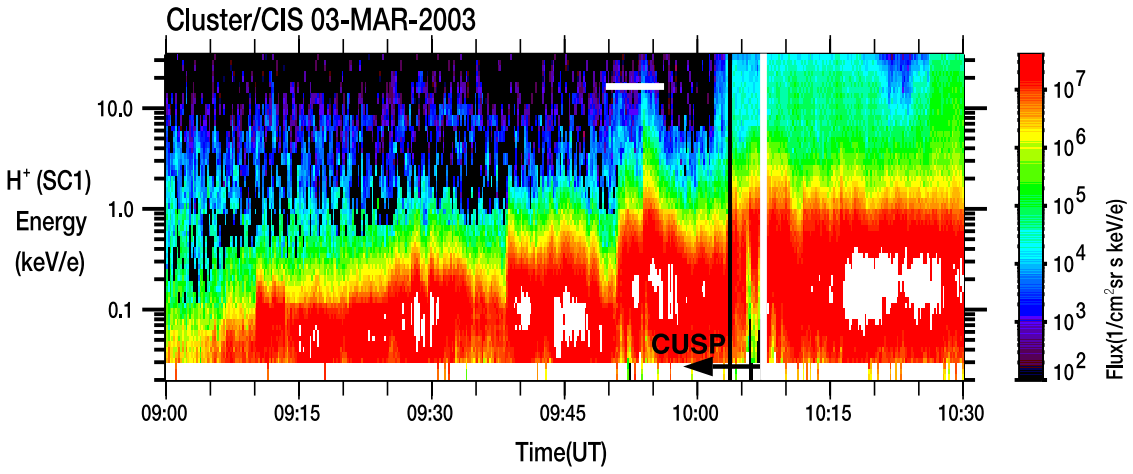

Figure 2. Cluster Ion Spectrometer (CIS) observations for the Northern Hemisphere cusp crossing on 3 March 2003. Plotted are H+ omnidirectional flux measurements (1/(cm2 s sr keV/e) for satellite SC1. Cluster crossed the cusp with increasing altitude toward lower magnetic latitudes and encountered a typical ion energy dispersion signature for southward IMF conditions, characterized by the time of flight effect. The cusp crossing is highly structured with sudden changes in the ion energy dispersion. The time period used for estimating the distance to the reconnection line is marked by a horizontal white bar.

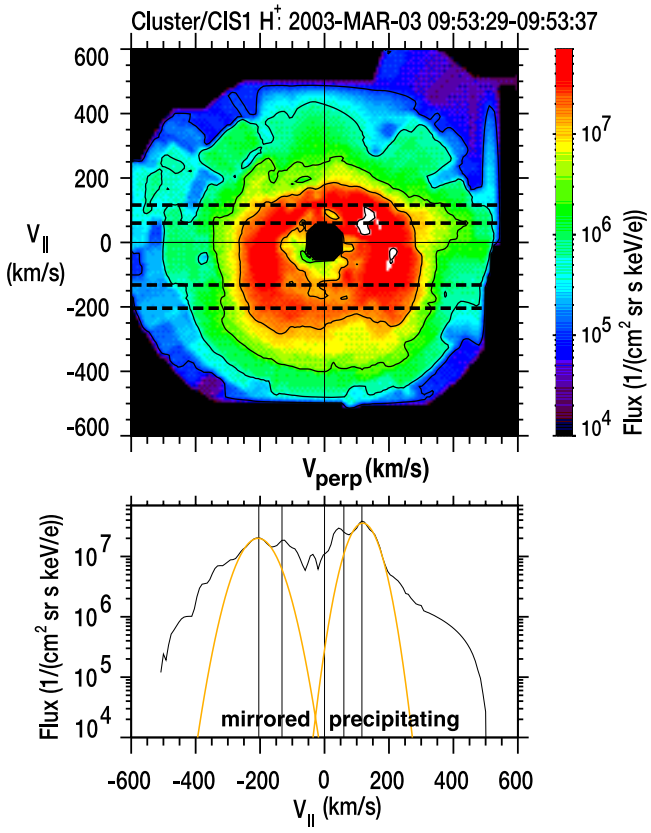

Figure 3. Two-dimensional cut of the three-dimensional distribution observed by Cluster/CIS instrument on board SC1. (top) The velocity space distribution in a plane containing the magnetic field (y-axis) and the plane perpendicular to the Sun-Earth line and (bottom) the one-dimensional cut of the distribution along the magnetic field direction. Precipitating magnetosheath ions moving along the magnetic field toward the ionosphere with a velocity of about 120 km/s (marked with a dashed line (top) and a solid line (bottom)) while the mirrored distribution from the ionosphere is observed at about −205 km/s. Additional lines in the two panels mark the 1/e cutoff velocities for the precipitating and mirrored distributions. Both distributions are fitted with Gauss distributions (yellow curve) to ensure consistent 1/e velocity cutoff definitions.

changes in the ion energy of the precipitating ions that are either caused by temporal variations of the reconnection rate [e.g., *Lockwood and Smith*, 1992; *Lockwood et al.*, 1998], changes in the reconnection location, or multiple reconnection lines [e.g., *Trattner et al.*, 2002a, 2003]. The cusp structures around 0950 UT with the highest ion energies are used to measure the low-velocity cutoffs in the precipitating and mirrored ion energy dispersions (marked by a horizontal white bar in Figure 2).

[23] Figure 3 (top) shows a two-dimensional cut through a three-dimensional distribution measured by the CIS instrument on board Cluster SC1 for the time interval from 0953:29 UT to 0953:37 UT on 3 March 2003. The distribution is plotted in the frame where the bulk flow velocity perpendicular to the magnetic field is zero. The plane of the two-dimensional cut contains the magnetic field direction (y axis) and the axis perpendicular to the Sun-Earth line. Three-dimensional flux measurements from the CIS instrument within ±45° of this plane are rotated into the plane by preserving total energy and pitch angle to produce the distribution in Figure 3 (top) [see also *Fuselier et al.*, 2000].

[24] Below the two-dimensional distribution is a cut through the distribution along the magnetic field direction. For both panels, distributions with positive velocities move parallel to the geomagnetic field toward the ionosphere, while distributions with negative velocities move away from the ionosphere, antiparallel to the geomagnetic field.

[25] The low-velocity cutoff method used to calculate the distance to the reconnection line for ion distributions observed inside the cusps is most reliable for widely separated precipitating and mirrored ion distributions. Owing to the velocity filter effect, ions with lower and lower velocities will arrive at the observing satellite at higher and higher latitudes, farther away from the open-closed field line boundary, thus bringing the precipitating and mirrored distributions closer together and subsequently merging the precipitating and mirrored distributions into one almost-isotropic distribution. The velocity-filter effect will make it impossible to observe low-velocity cutoffs for the precipitating and mirrored distribution far away from the open-closed field line boundary. Low-velocity cutoffs and therefore the distance to the reconnection site can be calculated most reliably close to the open-closed field line boundary at the edge of the cusp. For this reason, only the cusp structure with the highest ion energy in the Cluster CIS spectrogram was selected for the cutoff selection.

[26] The low-velocity cutoff is defined at the lower speed side of precipitating and mirrored ion beams where the flux is 1/e lower than the peak flux [see also *Fuselier et al.*, 2000; *Trattner et al.*, 2005]. To ensure a clear reproducible identification of the low-velocity cutoffs used for the distance calculation, the two-dimensional cuts of the Cluster/CIS observations are fitted with Gaussian distributions (yellow curves in Figure 3) that are subsequently used to define the 1/e reduced flux location.

[27] The precipitating magnetosheath distribution in Figure 3 has a distinct peak at about 120 km/s, while the peak of the mirrored magnetosheath distribution is located at about −205 km/s. Both peaks are marked with vertical solid lines (bottom) and horizontal dashed lines (top). Additional lines in Figure 3 represent the 1/e low-velocity cutoffs determined from the Gaussian fits of the distributions. The important consequence of the velocity filter effect is that protons near the low-velocity cutoffs in the parallel and antiparallel propagating populations originate near the reconnection site. The equal arrival times of the parallel and antiparallel propagating ions at these cutoffs and the known distance to the mirror point in the ionosphere are used to estimate the distance to the reconnection line (equation (1)).

[28] Figure 4 shows the distance to the reconnection line versus time for all the 8 s resolution Cluster/CIS 3D distributions during the 3 March 2003 cusp crossing, for which clearly separated low-velocity cutoffs could be observed. The distance to the reconnection site is relatively stable over the time interval with a weighted average distance of about 12.3 ± 1.7 R_E for this Cluster cusp crossing, while individual measurements vary over a range from about 9 to 16 R_E. Distance calculations are very sensitive to the low-velocity

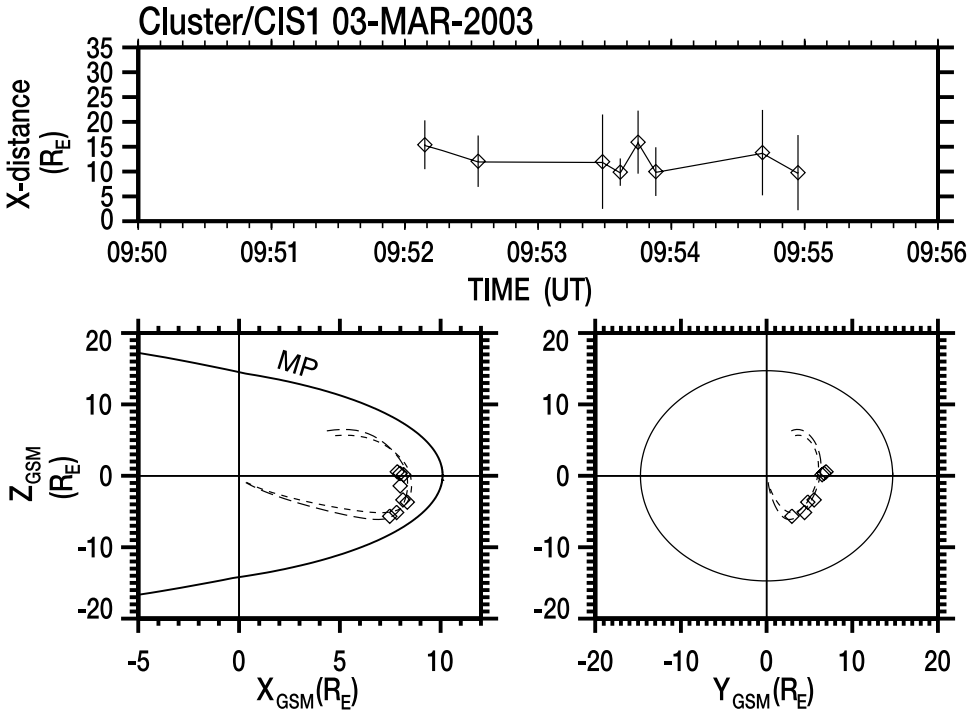

Figure 4. (top) The distance to the reconnection line for the Cluster SC1 Northern Hemisphere cusp crossing on 3 March 2003. (bottom) The location of the reconnection site at the magnetopause as seen from dawn (left) and from the Sun (right). The distances are traced along geomagnetic field lines from the T96 magnetic field model (dashed) starting at the position of the Cluster spacecraft SC1 in the magnetosphere towards the magnetopause (MP). The circle in the right panel represents the location of the magnetopause at the terminator plane.

cutoffs. The range of distances and the uncertainties in the distance to the reconnection site arises primarily from the uncertainties in measuring the low-velocity cutoffs. These uncertainties are defined as 1/2 the difference between the peak velocity and the low-velocity cutoff [e.g., *Fuselier et al.*, 2000].

[29] The bottom of Figure 4 shows the magnetopause as seen from the dawn sector (left) and the Sun (right). The circle in the right side of the figure represents the size of the magnetopause at the X = 0 plane separating the dayside magnetopause inside the circle from the tailside magnetopause outside the circle. Dashed lines represent two geomagnetic field lines from the T96 model, which starts at the position of the Cluster SC1 satellite in the northern cusp during the event. The diamond symbols are the location of the reconnection points derived from tracing the calculated distance in the top of Figure 4 along those field lines to the magnetopause. The reconnection line is located in the Southern Hemisphere in the dusk sector of the magnetopause.

[30] The magnetopause shear angle as seen from the Sun is shown in Figure 5. The circle in Figure 5 represents again the size of the magnetopause at the x = 0 plane. The magnetopause shear angle is calculated from the geomagnetic field direction and the IMF direction at the magnetopause. The geomagnetic field direction across the magnetopause was determined using the T96 field model at the *Sibeck et al.* [1991] magnetopause location for the solar wind conditions observed for the 3 March 2003 Cluster cusp crossing. To calculate the magnetopause shear angle, the IMF was draped around the magnetopause using the model by *Cooling et al.* [2001] that is based on the model by *Kobel and Flückiger* [1994]. The *Cooling et al.* [2001] magnetic field model is a restricted version of the more general Kobel and Flückiger model (which is an analytic representation of the magnetic field throughout the magnetosheath). The *Cooling et al.* [2001] analytic magnetic field model is valid only immediately outside of the magnetopause boundary. Like the Kobel and Flückiger model, the Cooling et al. model depends on the IMF and the magnetopause and bow shock standoff locations.

[31] Red regions represent antiparallel magnetic field regions at the magnetopause, while black regions represent parallel magnetic field conditions. Overlaid are the end points of the field line traces as seen in Figure 4 (bottom right) which are marked with square symbols and represent the location of the X-line at the magnetopause. For this Cluster cusp crossing, the location of the reconnection line is located close to the antiparallel reconnection region in the Southern Hemisphere.

[32] The white line in Figure 5 represents the location of a tilted X-line. The tilted X-line is determined by integrating away from the subsolar location, while maximizing the antiparallel component of the merging magnetic fields (similar to *Moore et al.* [2002] but generalized for nonzero dipole tilt angles). The tilted X-line model was first described by *Sonnerup* [1970]. As the magnetic fields, embedded within two separate regions and with a relatively

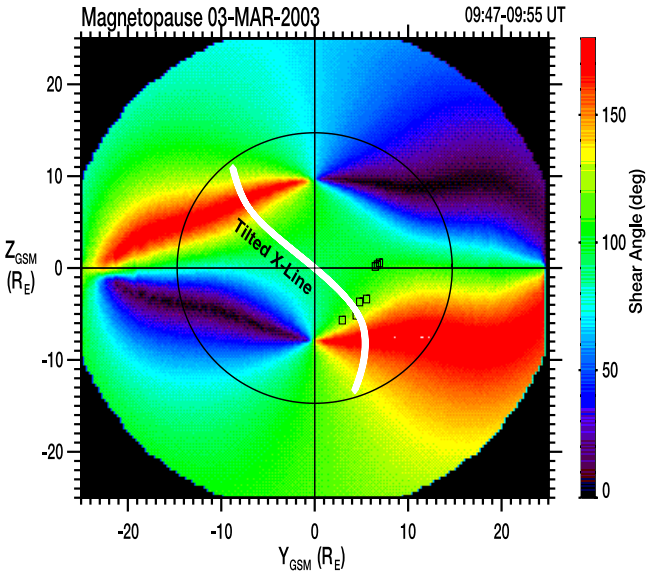

Figure 5. The magnetopause shear angle as seen from the Sun, based on the magnetic field direction of the T96 model and the IMF conditions at the magnetopause for the 3 March 2003 Cluster cusp crossing. The IMF was draped around the magnetopause using the model by *Cooling et al.* [2001]. The circle represents the magnetopause shape at the terminator plane. Square symbols represent the locations of the X-line at the magnetopause. The locations were determined by tracing the calculated distances to the X-line back along the geomagnetic field line in the T96 model, starting at the position of the Cluster SC1 satellite in the magnetosphere. The white line represents the location of the tilted X-line calculated for the magnetopause conditions during this Cluster cusp crossing.

large angle between them, approach, those locations where components of the magnetic fields are parallel and equal (guide field) define the orientation and location of the X-line. It was later noted by *Cowley* [1976] that, rather than the X-line being defined by the parallel components of the two different magnetic fields, the location of the X-line is determined by the places where components of the magnetic fields along the magnetopause are equal and opposite. The X-line orientation and location is then normal to these component directions (component reconnection). *Cowley and Owen* [1989] pursued this concept further along an idealized magnetopause surface with uniform and equal magnetic fields within each region, estimating also the resulting flux tube motion and energy transfer between the fields and plasma. The *Cowley and Owen* [1989] study has recently been further extended by *Moore et al.* [2002] to use a more realistic magnetospheric magnetic field (T96), and perfect draping of the IMF around the magnetopause boundary (i.e., clock angle is preserved). While the *Moore et al.* [2002] study focused on zero dipole tilt, we have extended this analysis by considering tilt angles commensurate with the actual time intervals of interest. In addition (as mentioned above), the draping of the magnetosheath field about the magnetopause is also more realistic (utilizing the *Kobel and Flückiger* [1994] model).

[33] Figure 6 shows H^+ omnidirectional flux measurements (1/(cm^2 s sr keV/e) for the Polar/TIMAS southern cusp crossings on 3 March 2003. Polar was located at about 76.9° ILAT, 5.7 R_E geocentric altitude and at 1248 MLT. The satellite was moving equatorward and crossed onto closed field lines at about 0130 UT. As during the first cusp crossing by Cluster, Polar encountered a typical ion energy dispersion with higher-energy ions arriving at lower latitudes, together with several sudden flux and energy changes in the ion-energy dispersion. However, the dispersion signature observed by Polar was considerably less pronounced than the dispersion signature observed by the Cluster

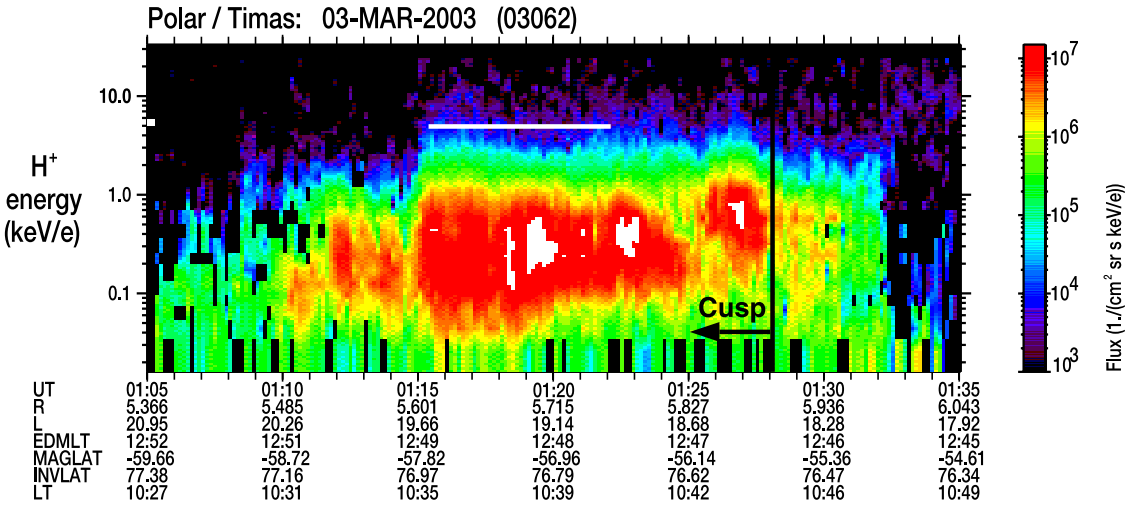

Figure 6. Polar Toroidal Imaging Mass-Angle Spectrograph observations for the Southern Hemisphere cusp crossing on 3 March 2003. Plotted are H+ omnidirectional flux measurements (1/(cm2 s sr keV/e)). Polar encountered downward precipitating magnetosheath ions at about 0110 UT and was moving equatorward towards closed field lines. The period of interest for estimating the distance to the reconnection line is marked by a white bar.

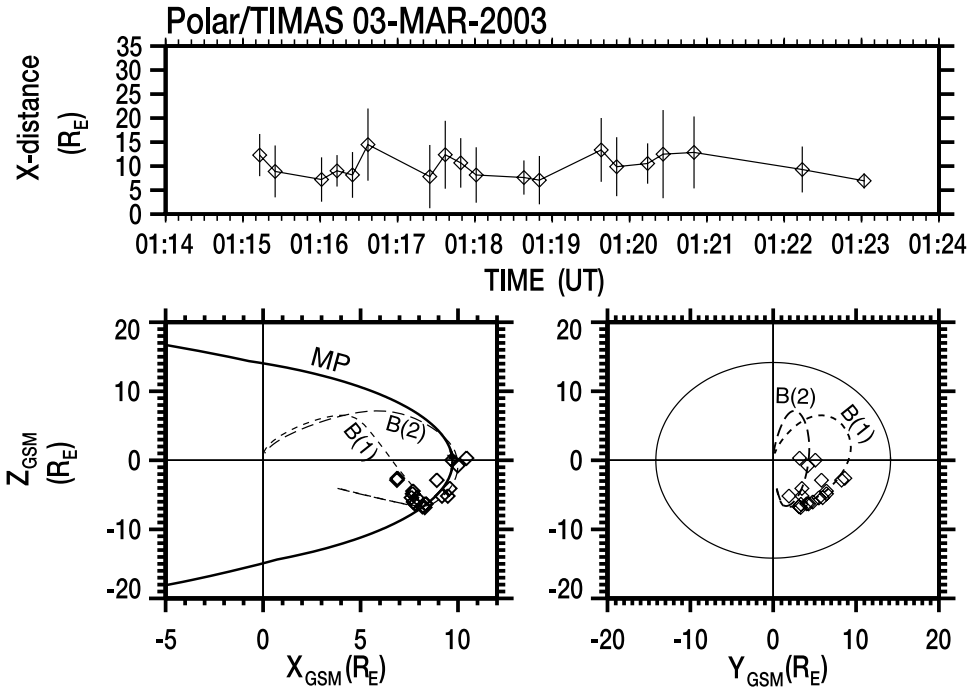

Figure 7. (top) The distance to the reconnection line for the Polar Southern Hemisphere cusp crossing on 3 March 2003. (bottom) The location of the reconnection site at the magnetopause as seen from dawn (left) and from the Sun (right). The distances are traced along geomagnetic field lines from the T96 magnetic field model (dashed) from the position of the Polar spacecraft in the magnetosphere toward the magnetopause (MP). The circle in the right side of the figure represents the location of the magnetopause at the terminator plane.

satellite in the Northern Hemisphere. The time of interest used for calculating the distance to the reconnection line is marked by a white bar.

[34] Figure 7 has the same layout as Figure 4 and shows the distance to the reconnection line versus time (top) for the 12-s Polar/TIMAS distributions that had discernable mirrored ion distributions during the southern cusp crossing on 3 March 2003. The distance to the reconnection site is again relatively stable over the time interval with a weighted average distance of about $8.6 \pm 0.9 R_E$, significantly shorter than the distance of the Cluster satellite from the reconnection site. Individual measurements of the Polar cusp trace vary between 6 and 14 R_E. The dashed lines in the bottom of the figure represent two geomagnetic field lines from the T96 model which starts at the positions of the Polar satellite in the southern cusp during the event. The diamond symbols are the location of the reconnection points derived from tracing the calculated distance in the top of the figure along those field lines to the magnetopause. The reconnection line is located in the Southern Hemisphere in the dusk sector of the magnetopause at the same location as the trace points from the Cluster northern cusp crossing.

[35] The magnetopause shear angle as seen from the Sun is shown in Figure 8. The format of Figure 8 is the same as that in Figure 5. The locations of the antiparallel and component reconnection sites at the magnetopause are very similar to the Cluster time interval due to the similarities in the IMF directions for both events. The antiparallel reconnection site is again located in the Southern Hemisphere of the afternoon sector. As before, the geomagnetic field line in the T96 model at the position of the Polar satellite is used to trace back each of the calculated distances to the reconnection site. The end points of these traces are marked with square symbols and overlaid in Figure 8 and represent the location of the X-line at the magnetopause. For this Polar cusp crossing the location of the reconnection line is located in the dusk sector of the Southern Hemisphere of the magnetopause, close to the antiparallel reconnection site in agreement with the location of the Cluster field line trace. Also indicated is the tilted X-line, which crosses the predicted location. The distribution of the reconnection points across the magnetopause with several locations along the tilted X-line at lower latitudes close to the equator and indicates that this reconnection event might be better represented by a tilted X-line and not by an antiparallel reconnection line.

4. Summary and Conclusion

[36] The location of the reconnection line at the magnetopause and its dependency on solar wind and IMF conditions is one of the major unsolved questions in magnetic reconnection and plasma entry into the magnetosphere [e.g., *Onsager and Fuselier*, 1994]. The three-dimensional capabilities of today's ion mass spectrometers like the TIMAS instrument on Polar or the CIS instruments on the European Cluster satellites can be used to estimate the location of the reconnection line at the magnetopause by applying the low-velocity cutoff technique. This technique has been successfully used with data obtained on a single spacecraft to

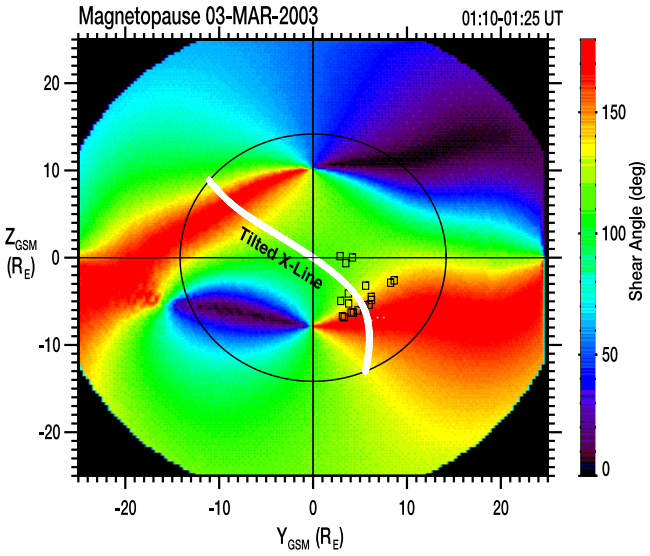

Figure 8. The magnetopause shear angle as seen from the Sun, based on the magnetic field direction of the T96 model and the IMF conditions at the magnetopause for the 3 March 2003 Polar cusp crossing. The IMF was draped around the magnetopause using the model by *Cooling et al.* [2001]. The circle represents the magnetopause shape at the terminator plane. Square symbols represent the locations of the X-line at the magnetopause. The locations were determined by tracing the calculated distances to the X-line back along the geomagnetic field line in the T96 model, starting at the position of the Polar satellite in the magnetosphere. The white line represents the location of the tilted X-line calculated for the magnetopause conditions during this Polar cusp crossing.

pinpoint the dayside magnetopause reconnection location in several statistical studies for northward IMF conditions in order to demonstrate the stability of the reconnection line at high latitudes [e.g., *Fuselier et al.*, 2000; *Petrinec et al.*, 2003] and to distinguish between antiparallel and component reconnection events [*Trattner et al.*, 2004]. In this paper we have extended the technique to use data acquired from two widely separated spacecraft. We analyzed cusp crossings by the Polar and Cluster satellites in the Southern and Northern Hemispheres, respectively, during very similar solar wind and IMF conditions. The difference between the IMF clock angles for the Polar and Cluster cusp crossings is just 8° with about the same dynamic pressure. These almost-conjugate events have been selected to demonstrate the robustness of the low-velocity cutoff method to determine the location of the reconnection line in preparation for a systematic study of the reconnection location at the magnetopause during southward IMF conditions.

[37] The low-velocity cutoff method is based on a time-of-flight model [e.g., *Onsager et al.*, 1990, 1991] and was first used in the Earth's plasma sheet boundary layer for the purpose of estimating the distance to the tailward reconnection site. The same principle can be applied by using the precipitating and mirrored cusp distributions together with the known distance between the observing satellite and the ionosphere. The calculated distance from the satellite to the reconnection site was subsequently traced back to the magnetopause along geomagnetic field lines from the T96 model, starting at the position of the cusp satellites. The shear angle at the magnetopause position of the reconnection line was derived from the fully draped IMF [*Cooling et al.*, 2001] and the T96 magnetic field model.

[38] The two cusp events in this study occurred on 3 March 2003, at 0110 to 0130 UT in the southern cusp (Polar) and 0900 to 1100 UT in the northern cusp (Cluster). The similarity in IMF clock angle for the two cusp events results in almost identical magnetopause shear-angle distributions with antiparallel reconnection regions in the dusk Southern and dawn Northern Hemispheres.

[39] The precipitating ions observed by the Polar satellite in the southern cusp originated in the dusk sector of the southern magnetopause close to the antiparallel reconnection region. The weighted average distance of the reconnection site from the Polar satellite was about $8.6 \pm 0.9 R_E$. The shear angle at that location was in the range from 120° to 140°.

[40] The precipitating ions observed by the Cluster SC1 satellite in the northern cusp were also traced to a reconnection site in the dusk sector of the southern magnetopause with a weighted average distance of about 12.3 ± 1.7 R_E. This reconnection location is in agreement with the Polar trace which demonstrates the ability of this technique to provide consistent results.

[41] While both trace locations are in the direct vicinity of the antiparallel reconnection region, this region is also crossed by the tilted X-line [*Cowley*, 1976] which makes a definitive decision between the two reconnection scenarios difficult. The distribution of the trace points at the magnetopause from the Polar cusp crossing, with several points located near the equatorial region, emphasizes a tilted X-line as the best representation to describe this reconnection event. More events with similar IMF clock angles at different MLT positions will be needed to confirm this conclusion.

[42] **Acknowledgments.** We acknowledge the use of the ISTP KP database. Observations of the interplanetary magnetic field were provided by the ACE Magnetic Field Instrument (MFI) [*Smith et al.*, 1998]. Solar wind observations were provided by the ACE Solar Wind Experiment (SWE) [*McComas et al.*, 1998]. The work at Lockheed Martin was supported by NASA contracts NAS5-30302, NAG5-12218, and NNG05GE93G. WKP is supported by NASA grant NNG05GE64G.

[43] Amitava Bhattacharjee thanks John C. Dorelli and another reviewer for their assistance in evaluating this paper.

References

Aubry, M. P., C. T. Russell, and M. G. Kivelson (1970), Inward motion of the magnetopause before a substorm, *J. Geophys. Res.*, *75*, 7018.

Cooling, B. M. A., C. J. Owen, and S. J. Schwartz (2001), Role of the magnetosheath flow in determining the motion of open flux tubes, *J. Geophys. Res.*, *106*, 18,763.

Cowley, S. W. H. (1976), Comments on the merging of nonantiparallel magnetic fields, *J. Geophys. Res.*, *81*, 3455.

Cowley, S. W. H., and C. J. Owen (1989), A simple illustrative model of open flux tube motion over the dayside magnetopause, *Planet. Space Sci.*, *37*, 1461.

Crooker, N. U. (1979), Dayside merging and cusp geometry, *J. Geophys. Res.*, *84*, 951.

Dungey, J. W. (1961), Interplanetary magnetic field and auroral zones, *Phys. Rev. Lett.*, *6*, 47.

Dungey, J. W. (1963), The structure of the ionosphere, or adventures in velocity space, in *Geophysics: The Earth's Environment*, edited by C. DeWitt, J. Hiebolt, and A. Lebeau, pp. 526–536, Gordon and Breach, New York.

Fairfield, D. H. (1971), Average and unusual locations of the Earth's magnetopause and bow shock, *J. Geophys. Res.*, *76*, 6700.

Fuselier, S. A., D. M. Klumpar, and E. G. Shelley (1991), Ion reflection and transmissions during reconnection at the Earth's subsolar magnetopause, *Geophys. Res. Lett.*, *18*, 139.

Fuselier, S. A., S. M. Petrinec, and K. J. Trattner (2000), Stability of the high-latitude reconnection site for steady northward IMF, *Geophys. Res. Lett.*, *27*, 473.

Fuselier, S. A., H. U. Frey, K. J. Trattner, S. B. Mende, and J. L. Burch (2002), Cusp aurora dependence on interplanetary magnetic field Bz, *J. Geophys. Res.*, *107*(A7), 1111, doi:10.1029/2001JA900165.

Fuselier, S. A., K. J. Trattner, S. M. Petrinec, C. Owen, and H. Reme (2005), Computing the reconnection rate at the Earth's magnetopause using two spacecraft observations, *J. Geophys. Res.*, *110*, A06212, doi:10.1029/2004JA010805.

Gosling, J. T., M. F. Thomsen, S. J. Bame, R. C. Elphic, and C. T. Russell (1990), Plasma flow reversal at the dayside magnetopause and the origin of asymmetric polar cusp convection, *J. Geophys. Res.*, *95*, 8073.

Gosling, J. T., M. F. Thomsen, S. J. Bame, R. C. Elphic, and C. T. Russell (1991), Observations of reconnection of interplanetary and lobe magnetic field lines at the high-latitude magnetopause, *J. Geophys. Res.*, *96*, 14,097.

Kobel, E., and E. O. Flückiger (1994), A model of the steady state magnetic field in the magnetosheath, *J. Geophys. Res.*, *99*, 23,617.

Lockwood, M., and M. F. Smith (1992), The variation of reconnection rate at the dayside magnetopause and cusp ion precipitation, *J. Geophys. Res.*, *97*, 14,841.

Lockwood, M., C. J. Davis, T. G. Onsager, and J. D. Scudder (1998), Modeling signatures of pulsed magnetopause reconnection in cusp ion dispersion signatures seen at middle altitudes, *Geophys. Res. Lett.*, *25*, 591.

Luhmann, J. R., R. J. Walker, C. T. Russell, N. U. Crooker, J. R. Spreiter, and S. S. Stahara (1984), Patterns of potential magnetic field merging sites on the dayside magnetopause, *J. Geophys. Res.*, *89*, 1739.

McComas, D. J., S. J. Blame, P. Barker, W. C. Feldman, J. L. Phillips, P. Riley, and J. W. Griffee (1998), Solar Wind Electron Proton Alpha Monitor (SWEPAM) for the Advanced Composition Explorer, *Space Sci. Rev.*, *86*, 563.

Moore, T. E., M.-C. Fok, and M. O. Chandler (2002), The dayside reconnection X line, *J. Geophys. Res.*, *107*(A10), 1332, doi:10.1029/2002JA009381.

Onsager, T. G., and S. A. Fuselier (1994), The location of magnetic reconnection for northward and southward interplanetary magnetic field, in *Solar System Plasmas in Space and Time*, *Geophys. Monogr. Ser.*, vol. 84, edited by J. L. Burch and J. H. Waite Jr., p. 183, AGU, Washington, D. C.

Onsager, T. G., M. F. Thomsen, J. T. Gosling, and S. J. Bame (1990), Electron distributions in the plasma sheet boundary layer: Time-of-flight effects, *Geophys. Res. Lett.*, *17*, 1837.

Onsager, T. G., M. F. Thomsen, R. C. Elphic, and J. T. Gosling (1991), Model of electron and ion distributions in the plasma sheet boundary layer, *J. Geophys. Res*, *96*, 20,999.

Onsager, T. G., C. A. Kletzing, J. B. Austin, and H. MacKiernan (1993), Model of magnetosheath plasma in the magnetosphere: Cusp and mantle particles at low altitudes, *Geophys. Res. Lett.*, *20*, 479.

Onsager, T. G., J. D. Scudder, M. Lockwood, and C. T. Russell (2001), Reconnection at the high-latitude magnetopause during northward interplanetary magnetic field conditions, *J. Geophys. Res.*, *106*, 25,467.

Petrinec, S. M., and S. A. Fuselier (2003), On continuous versus discontinuous neutral lines at the dayside magnetopause for southward interplanetary magnetic field, *Geophys. Res. Lett.*, *30*(10), 1519, doi:10.1029/2002GL016565.

Petrinec, S. M., K. J. Trattner, and S. A. Fuselier (2003), Steady reconnection during intervals of northward IMF: Implications for magnetosheath properties, *J. Geophys. Res.*, *108*(A12), 1458, doi:10.1029/2003JA009979.

Phan, T.-D., G. Paschmann, and B. U. Ö Sonnerup (1996), Low latitude dayside magnetopause and boundary layer for high magnetic shear: 2. Occurrence of magnetic reconnection, *J. Geophys. Res.*, *101*, 7817.

Phan, T.-D., et al. (2000), Extended magnetic reconnection at the Earth's magnetopause from detection of bi-directional jets, *Nature*, *404*, 848.

Reiff, P. H., T. W. Hill, and J. L. Burch (1977), Solar wind plasma injections at the dayside magnetospheric cusp, *J. Geophys. Res.*, *82*, 479.

Reme, H., et al. (2001), First multi-spacecraft ion measurements in and near the Earth's magnetosphere with identical Cluster ion spectrometry (CIS) experiment, *Ann. Geophys.*, *19*, 1303.

Rosenbauer, H., H. Grünwaldt, M. D. Montgomery, G. Paschmann, and N. Sckopke (1975), Heos 2 plasma observations in the distant polar magnetosphere: The plasma mantle, *J. Geophys. Res.*, *80*, 2723.

Shelley, E. G., R. D. Sharp, and R. G. Johnson (1976), He^{++} and H^{+} flux measurements in the day side cusp: Estimates of convection electric field, *J. Geophys. Res.*, *81*, 2363.

Shelley, E. G., et al. (1995), The toroidal imaging mass-angle spectrograph (TIMAS) for the Polar mission, *Space Sci. Rev.*, *71*, 497.

Sibeck, D. G., R. E. Lopez, and E. C. Roelof (1991), Solar wind control of the magnetopause shape, location, and motion, *J. Geophys. Res.*, *96*, 5489.

Smith, C. W., M. H. Acuna, L. F. Burlaga, J. L'Heureux, N. F. Ness, and J. Scheifele (1998), The ACE Magnetic Field Experiment, *Space Sci. Rev.*, *86*, 613.

Smith, M. F., and M. Lockwood (1996), Earth's magnetospheric cusp, *Rev. Geophys.*, *34*, 233.

Sonnerup, B. U. Ö. (1970), Magnetic field re-connection in a highly conducting incompressible fluid, *J. Plasma Phys.*, *4*, 207.

Sonnerup, B. U. Ö. (1974), The reconnecting magnetosphere, in *Magnetospheric Physics: Proceedings of the Advanced Summer Institute*, *Astrophys. and Space Sci. Library*, vol. 44, edited by B. M. McCormas, p. 23, Springer, New York.

Sonnerup, B. U. Ö., G. Paschmann, I. Papamastorakis, N. Sckopke, G. Haerendel, S. J. Bame, J. R. Asbridge, J. T. Gosling, and C. T. Russell (1981), Evidence for magnetic field reconnection at the Earth's magnetopause, *J. Geophys. Res.*, *86*, 10,049.

Trattner, K. J., S. A. Fuselier, W. K. Peterson, M. Boehm, D. Klumpar, C. W. Carlson, and T. K. Yeoman (2002a), Temporal versus spatial interpretation of cusp ion structures observed by two spacecraft, *J. Geophys. Res.*, *107*(A10), 1287, doi:10.1029/2001JA000181.

Trattner, K. J., S. A. Fuselier, W. K. Peterson, and C. W. Carlson (2002b), Spatial features observed in the cusp under steady solar wind conditions, *J. Geophys. Res.*, *107*(A10), 1288, doi:10.1029/2001JA000262.

Trattner, K. J., et al. (2003), Cusp Structures: Combining multi-spacecraft observations with ground based observations, *Ann. Geophys.*, *21*, 2031.

Trattner, K. J., S. M. Petrinec, and S. A. Fuselier (2004), The location of the reconnection line for northward IMF, *J. Geophys. Res.*, *109*, A03219, doi:10.1029/2003JA009975.

Trattner, K. J., S. A. Fuselier, S. M. Petrinec, T. K. Yeoman, C. Mouikis, H. Kucharek, and H. Reme (2005), The reconnection sites of spatial cusp structures, *J. Geophys. Res.*, *110*, A04207, doi:10.1029/2004JA010722.

Tsyganenko, N. A. (1995), Modeling the Earth's magnetospheric magnetic field confined within a realistic magnetopause, *J. Geophys. Res.*, *100*, 5599.

S. A. Fuselier, S. M. Petrinec, and K. J. Trattner, Lockheed Martin Advanced Technology Center, 3251 Hanover Street, B255, L9-42, Palo Alto, CA 94304-1191, USA. (trattner@mail.spasci.com)

W. K. Peterson, Laboratory for Atmospheric and Space Physics, University of Colorado, 1234 Innovation Drive, Boulder, CO 80303, USA.

H. Reme, Centre d'Etude Spatiale des Rayonnements, B.P. 4346, 9 Avenue du Colonel Roche, F-31028 Toulouse Cedex 4, France.